GRAVITY WAVES, UNBALANCED FLOW, AND AIRCRAFT CLEAR AIR TURBULENCE

Donald W. McCann

NOAA/National Weather Service
Aviation Weather Center
Kansas City, Missouri

Abstract

The "accepted" cause of clear air turbulence that plagues aircraft when flying at high altitudes is Kelvin-Helmholtz instability caused by wind shear. However, environmental Richardson numbers associated with aircraft turbulence reports are too high to assume that the turbulence is caused just by the environmental wind shear. Forecast techniques developed to date have assumed that there are layers of local Richardson number favorable for turbulence within the larger layer for which it was measured. The forecasts are probabilistic in the sense that the lower the environmental Richardson number, the more likely somewhere in the layer there will be turbulence. Theory and observations demonstrate that gravity waves can locally modify the wind shear and stability so as to produce turbulence. Analysis of model output associated with clear air turbulence events suggests that turbulence and indicators of large-scale atmospheric imbalance are related. Since highly unbalanced flow must undergo geostrophic adjustment which is a known cause of gravity waves, clear air turbulence may be caused by gravity waves. The conclusion, while preliminary, is that better clear air turbulence forecasts will likely come from an ingredients-based technique that includes both environmental wind shear and gravity wave forcing.

1. Introduction

Pilots have always had to consider the possibility of turbulence along their routes. Pilots expect turbulence near the ground, especially on windy, sunny days, and near weather systems such as fronts that produce phenomena such as rain showers or thunderstorms. As aircraft began flying at higher altitudes, they began encountering turbulence unexpectedly in regions without significant cloudiness, hence the name "clear air turbulence." CAT, as it is known, can be strong enough to cause significant injuries to passengers and crew when it is not expected. The news media has reported several of these events in recent years. However, when it is expected, occupants can be secured and objects can be stowed to minimize the damage. An outbreak of severe CAT over the Ohio Valley in the United States lasted an unprecedented three days (12-14 December 1997) with hundreds of aircraft and thousands of air travelers encountering the turbulence, yet no major damage or injuries were reported by the national media (Cundy 1999).

To date, CAT forecasting techniques have been an amalgamation of mostly empirical rules and equations (Dutton 1980; Knox 1997), most of which are based on connections between observed atmospheric patterns and aircraft turbulence reports. Doswell et al. (1996) summarized current thunderstorm forecasting techniques as being "ingredients-based." Simply put, there needs to be a favorable environment and a triggering mechanism in place for a thunderstorm to develop. This paper outlines a similar ingredients-based technique for CAT forecasting. The environmental setup can be measured by the vertical wind shear and the Richardson number. The triggers are gravity waves. While the technique is largely theoretical, reports from a CAT pilot report database are compared with diagnostics of wind shear and Richardson number and with diagnostics of unbalanced flow, a known cause of gravity waves. The results suggest that these ingredients are present in many cases. Environmental observations and numerical forecast model output is adequate to quantify wind shear and Richardson number. Much less is known about gravity waves produced from unbalanced flow. Quantifying this triggering mechanism requires much more theoretical and observational research.

2. Background

a. Richardson number

The generally accepted cause of CAT is Kelvin-Helmholtz instability (KHI) which occurs between two fluid layers that are statically stable but have sufficiently different velocities. The Richardson number is the ratio of static stability, as measured by the Brunt-Vaisala frequency (often designated as N) squared, and the wind shear squared:

$$Ri \equiv \frac{\frac{g}{\Theta}\frac{\partial \Theta}{\partial z}}{\left(\frac{\partial V}{\partial z}\right)^2} \tag{1}$$

The notation of this and all subsequent equations is defined in the appendix.

There is a special relationship of turbulence to the Ri. Because the denominator is always positive, when the stability is negative, i.e., the lapse rate is superadiabatic, Ri < 0.0 and convective turbulence can develop. When 0.0 < Ri < 0.25, KHI can form, and when Ri > 0.25, KHI cannot form. This critical Richardson number can be shown

theoretically (Miles and Howard 1964) and experimentally (Thorpe 1969) as a threshold below which an atmosphere may be turbulent. Stabilities and wind shears as measured by standard rawinsonde observations yielding Richardson numbers less than 0.25 are common in the boundary layer (McCann 1999). Above the boundary layer where CAT occurs, Ri values less than 0.25 have been observed in thin layers by special observations (Browning et al. 1970; Reed and Hardy 1972) but are rarely observed by standard rawinsondes (Murphy et al. 1982). Because layers with Ri < 0.25 should quickly become turbulent and raise Ri to more stable values, it is by chance when a rawinsonde observes one.

Numerous researchers in the 1960s and early 1970s recognized that customary atmospheric observations were too coarse to observe the stabilities and wind shears that result in low Ri values and CAT. As a group, they made an implicit assumption that the lower the environmental Richardson number (Ri_E), the more likely that somewhere within that thick layer, there were thin layers of local Richardson number (Ri_L less than the critical value (e.g., Roach 1970). Since in many cases it was high environmental wind shear that lowered Ri_E, quoting from Knox (1997b), "The mystery of CAT was thought to be solved when its connection to vertical shear instabilities was discovered (Dutton and Panofsky 1970)." Forecast techniques from that era stressed analysis of Ri_E, especially the vertical wind shear portion. For example, Roach (1970) derived a Ri_E tendency equation. Even the more recent Ellrod and Knapp (1992) index of wind shear times deformation is wind shear-based. Frontogenetic deformation can cause the large-scale wind shear to increase through the thermal wind relationship, and it was the rationale in including it in their index. Knox (1997b) analyzed the theory underlying these methods and found it incomplete since other dynamic processes can also increase environmental wind shear.

b. Turbulent kinetic energy

Turbulent kinetic energy (TKE) equations are the basis for understanding turbulence in the atmospheric boundary layer (McCann 1999). Since they are based on the equations of motion, they should also be applicable to the free atmosphere. The simplest is a steady-state first order closure equation in which the turbulence is assumed to be analogous to diffusion, i.e., the turbulent flux of any quantity is proportional to the mean gradient of the quantity being transferred (Garratt 1992):

$$\varepsilon = K_m\left(\frac{\partial V}{\partial z}\right)^2 - K_h\frac{g}{\Theta_v}\frac{\partial \Theta_v}{\partial z} \qquad (2)$$

This relationship is known as the flux-gradient TKE equation or K-closure equation because of the proportionality constants K_m and K_h. The term on the left-hand side of (2) is the TKE dissipation due to molecular viscosity while the two terms on the right-hand side are TKE production terms due to wind shear and stability. Because the turbulent fluxes are assumed to be downgradient, K_m and K_h are positive.

The Richardson number as an indicator of turbulence can only discriminate between turbulent and non-turbulent environments. It does not give any indication of how strong the turbulence is. On the other hand, with the TKE equation one can compute not only a yes/no answer for turbulence, based on positive or negative TKE production, but also the amount of turbulence, based on the quantity of positive TKE production. However, in order to apply the TKE equation to the aircraft turbulence problem, one has to assume that turbulence dissipation at the molecular level (ϵ) cascades from larger turbulent eddies. Vinnichenko et al. (1980) note that turbulence felt by an individual aircraft is from air gusts associated with eddies in a size range that is a function of aircraft performance factors such as design and speed. Aircraft cannot feel turbulence from small eddies, and they tend to ride with larger eddies. For most aircraft, eddies on the order of 100 m affect them the most. Turbulent intensities from aircraft observations and TKE dissipation have been related in some studies (MacCready 1964; Lester and Fingerhut 1974; McCann 1999), so to use TKE production/dissipation to diagnose/forecast turbulence is a credible hypothesis.

When modeling atmospheric flows, it is important to include the turbulence. Modelers parameterize the turbulence that occurs in the thin layers between the thick model layers by the K-values. The parameterization accounts for the mean turbulence within the model layer. Straightforward algebraic manipulation of this TKE equation (McCann 1999) shows that

$$\varepsilon = K_h\left(\frac{\partial V}{\partial z}\right)^2\left(\frac{K_m}{K_h} - Ri\right) \qquad (3)$$

The ratio of the eddy viscosity (K_m) to the eddy thermal diffusivity (K_h) is called a turbulent Prandtl number (Pr). Inspecting (3), only when Ri < Pr will the TKE production be positive. Since the Richardson number must be no higher than 0.25 for turbulence to begin, it follows that the Prandtl number should be equal to the critical Richardson number of 0.25 if positive TKE production is related to the occurrence of turbulence. However, if the turbulence is occurring in layers between the model layers – and it always does, a higher Prandtl number is necessary to parameterize the turbulence. Mellor and Yamada (1982) suggest Pr $\approx$ 0.8 for numerical modeling of atmospheric boundary layers. Estimating K_m and K_h independently in a number of cases of aircraft observed wind shears and stabilities in turbulent upper tropospheres, Kennedy and Shapiro (1980) computed a range of Pr from 0.9 to 5.5 and recommended values in this range to parameterize turbulence in operational numerical models.

One must be careful in choosing a Prandtl number to use in the TKE equation as a CAT forecast technique. Turbulence becomes more intermittent as Ri_E increases above 0.25 (Kondo et al. 1978). Thus with increasing Ri_E an aircraft is less and less likely to encounter a turbulent eddy. Therefore, the existence of turbulence is a probabilistic function of Ri_E, and the chosen Prandtl number defines a threshold Richardson number (Ri_{max}) which is

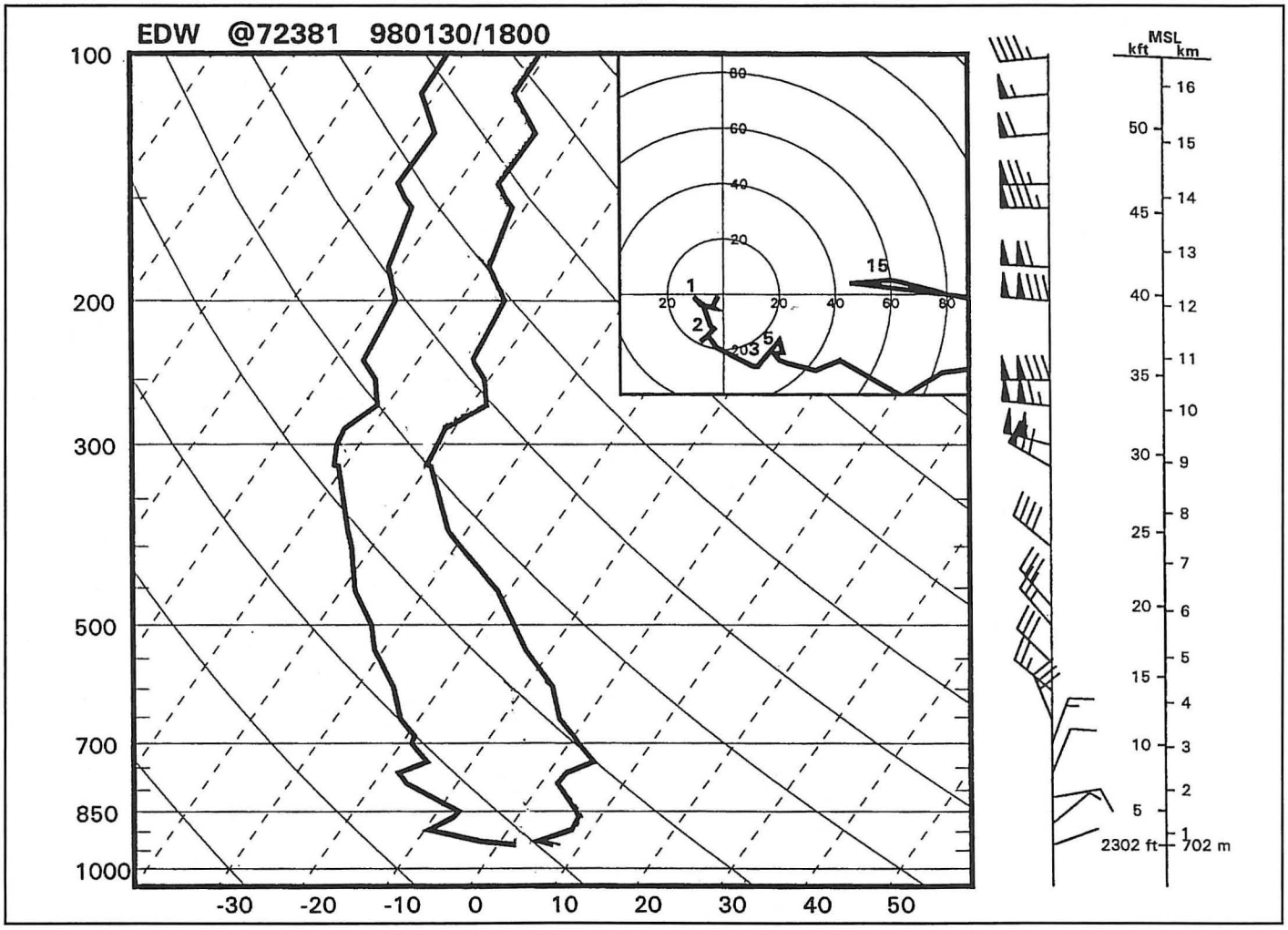

Fig. 1. Rawinsonde measured sounding at Edwards Air Force Base, California, 1800 UTC 30 January 1998. The temperature and dew point temperature profiles are displayed on a standard Skew-T/log p diagram. Winds (in knots) are plotted to the right of the display. A hodograph of the winds is in the upper right. A standard atmosphere height scale is located to the right of the winds.

the upper limit of Ri_E in which the probability is greater than zero, the lower limit of $Ri_E = 0.25$ being 100% probability. Since the mean TKE is quantitative, the higher the Ri_{max}, the weaker the relation between the probability of turbulence and its mean intensity. The mean TKE may be the integration of a large number of small turbulence events or of a small number of large turbulence events. The latter is far more important to aircraft turbulence forecasting than the former. Ideally, the Ri_{max} should be 0.25 so the probability of turbulence with $Ri < 0.25$ is near 100%.

3. Gravity Wave Modification of Wind Shears and Stabilities

The closer one can estimate Ri_L in (3), the closer one can set Ri_{max} to 0.25 and have greater confidence in (3) as an aircraft turbulence forecast tool (McCann 1999). A gravity wave is one mechanism that locally modifies Ri_E. Kondo et al. (1978) noted that the turbulence intermittency at $Ri_E > 0.25$ was due to gravity waves. The theory of how gravity waves locally increase wind shear and reduce stability have been known for many years (Roach 1970).

Consider the following pilot report received at the Aviation Weather Center (AWC) on 30 January 1998:

> LAX UUA /OV LAX-LAX 050050/TM 1806/ FL325/TP B767/SK CLR/WV 290/250046 320/ 256140 330/260146/TB DURC LAX SMTH 290-320 MDT SMTH ABV/ RM STG SHR 290-320

Heights are given in hundreds of feet above sea level and winds in knots. The turbulence group (TB) decodes as smooth during climb out of Los Angeles, California, (LAX) except for moderate turbulence between 29,000 feet and 32,000 feet (8800 m to 9800 m). Winds (WV) measured by this modern aircraft's (Boeing 767) inertial navigation system are typically very accurate and show a large increase from 250 degrees/46 knots (24 m sec^{-1}) to 256 degrees/140 knots (72 m sec^{-1}) in the layer within which the turbulence occurred.

Compare the aircraft's observed winds with those shown in Fig. 1 which are from a rawinsonde observation launched at Edwards Air Force Base, California, (EDW) just 40 km to the northwest of the aircraft's location about the same time as the pilot report. The winds at

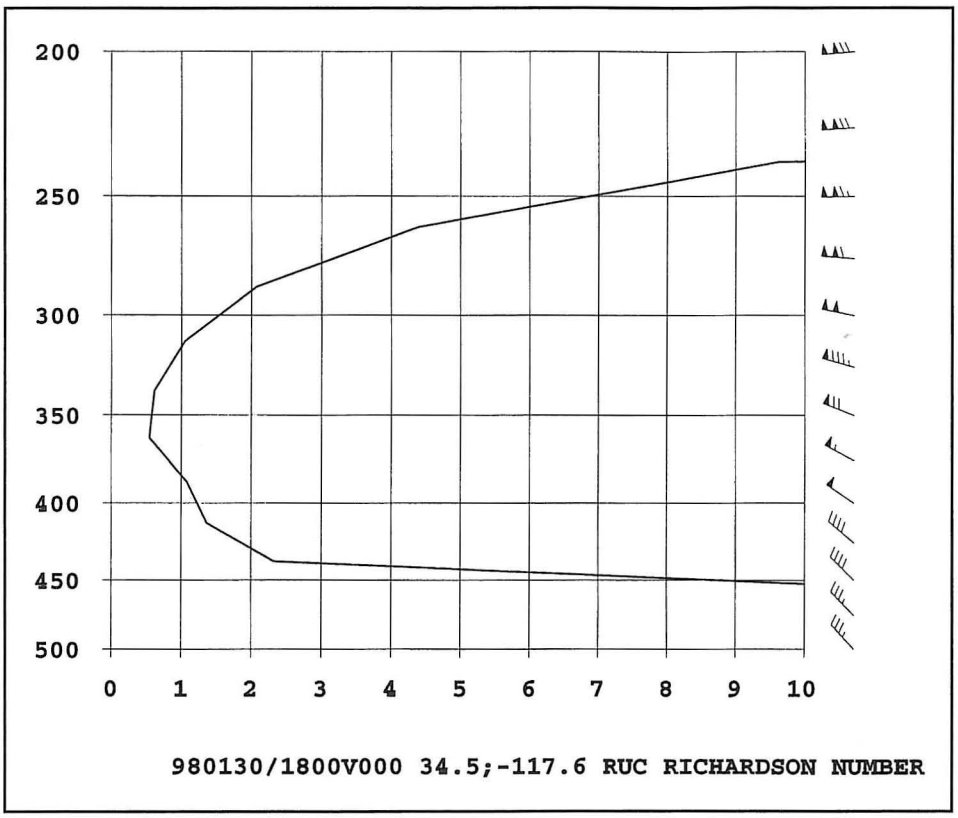

Fig. 2. A vertical profile of the Richardson number between 500 mb and 200 mb from the 1800 UTC 30 January 1998, Rapid Update Cycle numerical model at a location approximately 50 nautical miles northeast of Los Angeles, California. This is near the location of the aircraft in the pilot report in the text. The 350-mb level is about 27,000 feet (8200 m) MSL; the 300-mb level is about 30,000 feet (9100 m) MSL; and the 250-mb level is about 34,000 feet (10,400 m) MSL.

29,000 feet are from about 285 degrees/70 knots (36 m sec^{-1}), not the 250/46 knots reported by the aircraft. The winds at 32,000 feet are about 275 degrees/115 knots (60 m sec^{-1}) on the rawinsonde and 256/140 knots from the aircraft. The vertical shear from the aircraft is more than three times that from the rawinsonde.

Since the difference between these observations is much greater than the known errors expected for either system (Schwartz and Benjamin 1995), one must conclude that each observation recorded a different wind pattern even though both were taken in close proximity of each other. The 1800 UTC Rapid Update Cycle (RUC) wind analysis at the location of the aircraft shown in Fig. 2 is similar to the rawinsonde's. The aircraft reported SMOOTH at the lowest Ri_E near the 27,000 foot (8200 m) flight level.

The wind shear measured by the aircraft may have been enhanced by a gravity wave. Using the dispersion relation for the vertically propagating component of the wave, Palmer et al. (1986) and Dunkerton (1997) derived the wave's impact on the local vertical shear in a non-

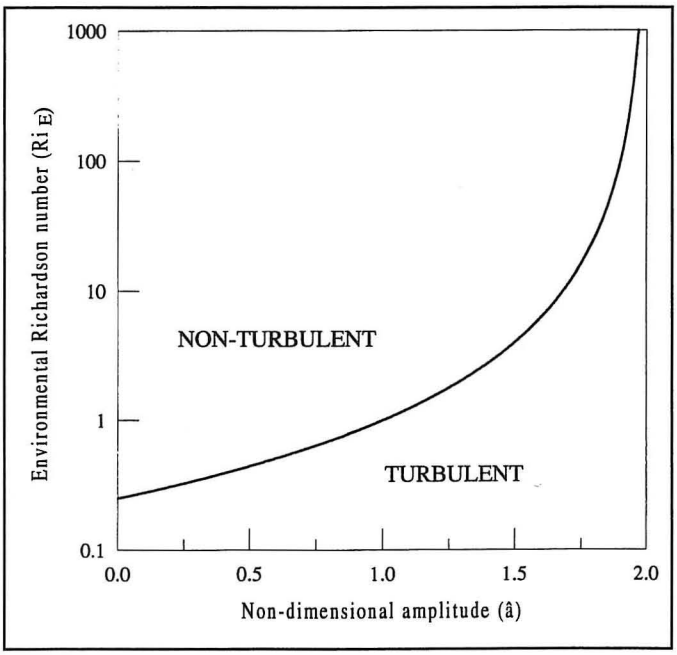

Fig. 3. Curve of the bounding value of the environmental Richardson number as a function of the non-dimensional amplitude (â). When (â, Ri_E) falls in the TURBULENT region, a gravity wave will locally increase the wind shear sufficiently to reduce the local Richardson number to 0.25.

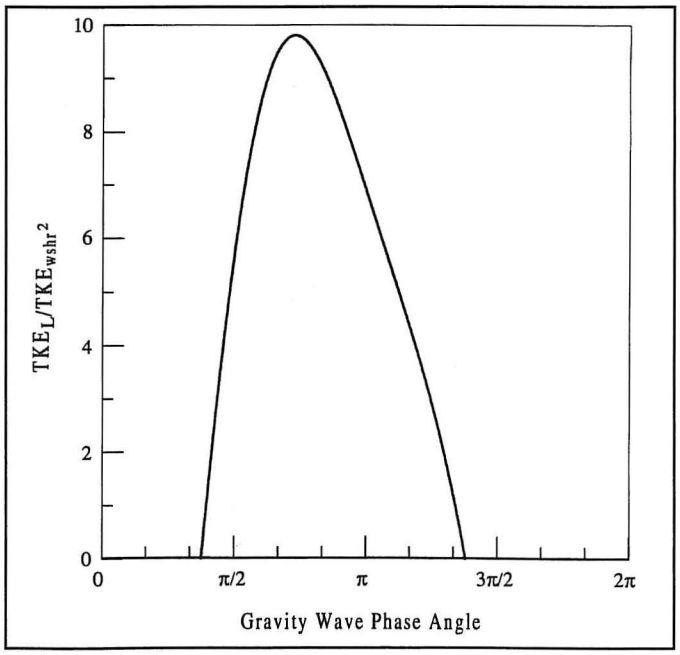

Fig. 4. The ratio of the total local TKE production to the TKE production by the environmental wind shear as computed for the 30 January 1998 case of the B767 aircraft ascent out of Los Angeles, California, using equation (2) in the text. The wind shear and stability were modified using Eqs. (4) and (5) with a = 1.98. The turbulent Prandtl number, $K_m/K_h = 0.25$.

rotating environment:

$$\left(\frac{\partial V}{\partial z}\right)_L = \left(\frac{\partial V}{\partial z}\right)\left(1 + Ri_E^{1/2}\hat{a}\sin\phi\right) \quad (4)$$

and the wave's impact on the local stability:

$$N_L^2 = N^2\left(1 + \hat{a}\cos\phi\right) \quad (5)$$

The non-dimensional amplitude, $\hat{a} = Na / |V\text{-}\mathbf{c}|$ (where a is the actual amplitude of the wave) is an inverse Froude number. The denominator is the Doppler-adjusted wind velocity where **c** is the phase velocity of the wave (Dunkerton 1997). When $\hat{a} > 1.0$, wave overturning begins. The nondimensional amplitude will be high when any of three environmental variables are sufficiently favorable, 1) high gravity wave amplitude, 2) high stability, and 3) low difference between the wind and the wave velocities. When the wind velocity equals the wave velocity, the wind is said to be at a "critical" value with respect to the wave (Dunkerton 1997). The gravity wave phase angle, ϕ, locates where in the gravity wave the changes of stability and shear are taking place. In a gravity wave both the stability and shear fluctuate around their environmental values, sometimes increasing them and sometimes decreasing them. Equations (4) and (5) can be combined into a locally adjusted Richardson number under the influence of the gravity wave.

$$Ri_L = Ri_E \frac{1 + \hat{a}\cos\phi}{\left(1 + Ri_E^{1/2}\hat{a}\sin\phi\right)^2} \quad (6)$$

When $\phi = \pi$ and $\hat{a} > 1$, it follows from (6) that $Ri_L < 0.0$, so when waves break, the stability can be negative and cause convective turbulence. When $\phi = \pi/2$, wind shear is maximized; it again follows from (6) that $Ri_L < 0.25$ when $Ri_E^{1/2}(2\text{-}\hat{a}) < 1$. For $\hat{a} > 2$, Ri_L is always less than 0.25. When $\hat{a} < 2$, it is necessary for Ri_E to be below a certain value in order to lower Ri_L to below 0.25. That value is a function of the non-dimensional amplitude. As $\hat{a} \rightarrow 2$, the upper limit on Ri_E for turbulence approaches infinity. Figure 3 depicts the graph of this curve. Below the curve are Ri_E and nondimensional amplitude combinations that are turbulent.

In fact, $\hat{a}$ can be computed for the 30 January 1998 turbulence event above if it were caused by a gravity wave. Since Ri_E (1.5) and the environmental wind shear (.0155 sec^{-1}) are known, and assuming the wind shear measured by the aircraft (.0531 sec^{-1}) is the maximum ($\phi = \pi/2$), (4) can be solved for $\hat{a}$. In this case $\hat{a} = 1.98$. Although the environmental conditions are unfavorable for turbulence ($Ri_E = 1.5$), the nondimensional amplitude is so high that a portion of the wave would be turbulent due to convective instability and a portion due to shear instability. The maximum local TKE production due to the gravity wave relative to that from environmental wind shear can be computed by assuming a conservative 4:1 ratio of K_h to K_m, i.e., Pr = 0.25, using $\hat{a} = 1.98$ in (4) and (5), and then using those values in (2). From Fig. 4, the maximum local TKE production is almost 10 times that of environmental wind shear. This is realizable TKE production, not TKE production that is reduced by stability. In this case about half the wave is turbulent ($Ri_L < 0.25$).

The basic assumption underneath current CAT forecast techniques becomes clearer. The lower the environmental Richardson number, the higher the probability that a gravity wave with sufficient non-dimensional amplitude will reduce the local Richardson number to less than 0.25. The environmental wind shear's role is also clear. The environmental wind shear and the maximum local wind shear after gravity wave modification are directly proportional to each other. Therefore, for a given Ri_E and $\hat{a}$, a high environmental wind shear will translate into more TKE production than a low environmental wind shear. Therefore, the current CAT forecasting techniques have only been examining one part of the CAT problem, the environmental setup. A more complete technique will have to examine the potential for triggers.

4. Unbalanced Flow Indicators

If gravity waves trigger CAT in the manner described in the previous section, then improving CAT diagnostics requires knowledge of the gravity waves that cause the CAT. There are many sources of gravity waves; mountains, thunderstorms, and unbalanced flow are examples (Kaplan et al. 1997). Turbulent Kelvin-Helmholtz waves and other gravity wave breaking may even cause more gravity waves (Franke and Robinson 1999). Any gravity wave may be a potential turbulence producer.

Knox (1997b) suggested that geostrophic adjustment and inertial instability have been overlooked as a possible cause of CAT. Whenever forces are unbalanced, geostrophic adjustment excites gravity waves. First noted by Rossby (1938), these waves have been examined by a number of researchers theoretically (e.g., Cahn 1945 and Weglarz and Lin 1997), mathematically (e.g., Blumen 1972, Duffy 1990, and Fritts and Luo 1992), and with simple numerical models (e.g., van Tuyl and Young 1982 and O'Sullivan and Dunkerton 1995). Table 1 is a list of some of the diagnostics that authors have used to identify regions of unbalanced flow.

The first on the list is the inertial advective wind. Uccellini et al. (1984) noted that jet streak regions with ageostrophic parcel motions could be identified as regions of significant momentum change. In their case study they computed a Rossby number

$$Ro \approx \frac{|V \cdot \nabla V|}{f|V|}$$

which is an approximation of the usual Ro (ratio of advective to Coriolis forces) which neglects the local tendency of **V**. They found that it approaches unity in regions with the largest unbalanced flow. Note that the inertial advective wind defined in Table 1 is the Rossby number multiplied by the wind speed. Many times the Rossby number becomes large in slow flow. Even though in those cases there is a relative imbalance of forces, the absolute imbal-

Table 1. Unbalanced flow diagnostics and their sources.

NAME	FORMULA	SOURCE
Inertial Advective Wind	$V_{inad} = \frac{\lvert V \cdot \nabla V \rvert}{f}$	Uccellini et al. (1984)
Unbalanced Ageostrophic Wind	$V_{uage} = \sqrt{\lvert V \rvert^2 - \left(V_g \cdot V_{ag}\right)^2}$	Koch and Dorian (1988)
Divergence Tendency	$\frac{dD}{dt} = -\nabla^2\Phi + 2J(u,v) + f\zeta - \beta u$	Zack and Kaplan (1987)
Anticyclonic Instability	$\left(\zeta + f\right)\left(\zeta_{curv} + \frac{f}{2}\right) < 0$	Alaka (1961)

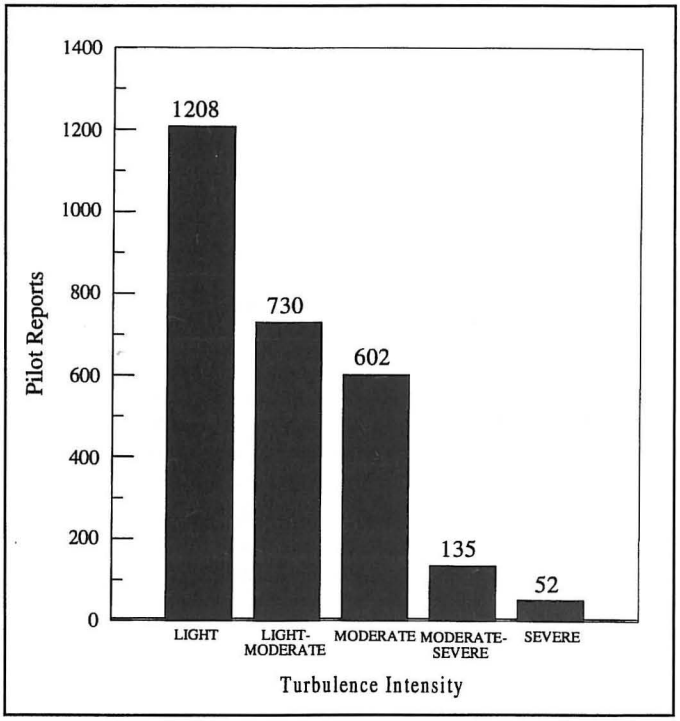

Fig. 5. The distribution of the AWC database pilot report turbulence greater than a particular intensity.

ance of weak forces in these cases is small which should lead to weak gravity wave production.

Koch and Dorian (1988) introduced the second unbalanced flow indicator in the Table 1 list. Their study connected the source of a mesoscale gravity wave event with a region of unbalanced flow. The indicator they chose to compute was an unbalanced ageostrophic Rossby number which is the ratio of the component of the ageostrophic wind normal to the flow to the wind speed itself. For the same reason as above, the unbalanced ageostrophic wind in Table 1 is their Rossby number multiplied by the wind speed.

The third unbalanced flow indicator has a long history. It is derived from taking the horizontal divergence of the equation of horizontal motion. When dD/dt = 0, the equation is sometimes known as the nonlinear balance equation. Charney (1955) noted that when the divergence tendency is zero everywhere, the wind and the mass fields are in balance, and the integration of primitive equations in early numerical models could proceed without getting unwanted gravity waves. Uccellini and Koch (1987) and Zack and Kaplan (1987) showed how significant divergence growth leads to unbalanced flow.

Knox (1997a) discussed sources of unbalanced flow in anticyclonic flow, that is inertial instability and gradient flow non-ellipticity. The former is the familiar instability of negative absolute vorticity (in the Northern Hemisphere). The latter occurs when winds are "anomalous," or high enough to produce imaginary solutions to the quadratic gradient wind equation. Alaka (1961) derived a general anticyclonic instability criterion on an isentropic surface that is the product of these two "instabilities." The listing in Table 1 is somewhat of a simplification of that criterion in that the curvature vorticity is computed on "level" pressure surfaces and with streamline curvatures instead of trajectory curvatures. In most cases, these simplifications will overestimate the negative curvature vorticity. As the subsequent results will show, these simplifications do not seem to hurt this index as an unbalanced flow/turbulence indicator.

5. Observations of Unbalanced Flow Indicators and Turbulence

Environmental Richardson numbers, wind shears, and the above unbalanced flow diagnostics were computed for each of 1832 pilot reports above the 20,000 foot (6100 m) flight level in a database gathered every workday from 1 October 1996 to 31 January 1997. The AWC receives hundreds of turbulence pilot reports each day. Pilot reports are notorious for low quality and cannot be automatically processed with sufficient quality control (Schwartz 1996). In order to manage this large volume and to ensure that the reports were of high quality, the pilot reports were manually sampled. Every three hours (0000 UTC, 0300 UTC, etc.) available reports over the contiguous United States plus or minus one hour of the observation time were added to the database in this manner: all reports SEVERE or MODERATE-SEVERE, one MODERATE or LIGHT-MODERATE, one LIGHT, and one SMOOTH. If more than ten MODERATE reports occurred in the period, then one additional report was added. Reports MODERATE or less were chosen randomly. Care was taken to make certain of a pilot report's details and to exclude reports in known thunderstorms or mountain waves. Included are reports of "chop," which, in a pure sense, is not turbulence but is often mistakenly reported in turbulent conditions. The goal was to sample the environmental conditions of all turbulence intensities in order to discern their differences. The database is not a statistical sample of all turbulence pilot

Table 2. Postagreement Richardson number and wind shear squared (foundations of traditional CAT diagnostics) and of various unbalanced flow diagnostics with MODERATE or greater turbulence pilot reports. The statistics are based on 1832 "randomly" selected pilot reports of turbulence above 20,000 foot (6100 m) flight level between I October 1996 and 31 January 1997. The number to the right of each slash is the number of times the value of the unbalanced flow diagnostic exceeded the threshold. The number to the left of the slash is the number of those pilot reports exceeding the threshold with turbulence intensities MODERATE or greater.

Richardson number (Ri_E)	
< 3	235/430 = .55
< 2	159/242 = .66
< 1	65/78 = .83
< 0.5	5/6 = .83
Wind shear squared ($wshr^2$)	
> .0001 sec^{-2}	250/419 = .60
> .00025	108/170 = .64
> .0005	36/49 = .73
> .00075	13/14 = .93
Inertial Advective Wind (Inadwind)	
> 15 knots	215/354 = .61
> 25	82/125 = .66
> 35	31/48 = .65
> 45	18/24 = .75
> 55	10/13 = .77
Unbalanced Ageostrophic Wind (Uagewind)	
> 15 knots	215/536 = .40
> 25	66/151 = .44
> 35	25/53 = .47
> 45	10/16 = .62
> 55	6/7 = .86
Divergence Tendency (Divgtend)	
> 10 ($x10^{-9}$) sec^{-2}	163/218 = .75
> 15	77/90 = .86
> 20	35/43 = .82
> 25	12/14 = .86
> 30	5/5 = 1.00
Anticyclonic Instability (AI)	
< 0 ($x10^{-10}$) sec^{-2}	30/49 = .61
< -5	14/21= .67
< -10	8/9 = .89
<-15	3/3 = 1.00

reports. Figure 5 shows the number of pilot reports in the database greater than a particular intensity. The environmental data came from the matching three hourly Rapid Update Cycle (RUC) model analysis of winds and temperatures at every 25 mb pressure level.

Table 2 displays how many reports in the database were inside a contour of a particular value and how many of those reports were MODERATE or greater turbulence.

These statistics estimate a postagreement or frequency of hits ratio (one minus the false alarm rate [FAR]) for each diagnostic. A high value indicates that the diagnostic is good in the sense that if the threshold is exceeded, it means the phenomenon will likely occur. The higher the postagreement, the more likely the diagnostic has a physical relation with the phenomenon.

Although the thresholds for Ri_E show a high postagreement as one would expect from the theory presented in Section 2, the $Ri_E = 3.0$ threshold is not very useful for diagnosis or forecasting MODERATE turbulence because it overforecasts the turbulence intensity (Rockey and McCann 1995). The thresholds for wind shear squared also show high postagreement as expected.

Of the four unbalanced flow diagnostics, the divergence tendency appears to have the highest skill in finding the significant turbulence pilot reports in the database. Values of 10×10^{-9} sec^{-2} are only moderately high values of divergence tendency based on everyday analyses at the AWC, yet a very high percentage of turbulence reports were MODERATE or greater whenever they occurred within this contour. Negative anticyclonic stability also shows high postagreement. With a low number of occurrences, this diagnostic is not triggered very often, but when it happens, it is comparable to the divergence tendency. The inertial advective wind and the unbalanced ageostrophic wind show less but still fair postagreement. These results suggest that these may not be optimally formulated. Indeed, there are simplifying assumptions in both their derivations (Uccellini et al. 1984 and Koch and Dorian 1988). The divergence tendency and Alaka's (1961) criterion are more fundamental to the idea of imbalance than the others.

Do the different diagnostics catch different events? Table 3 shows the percentage of MODERATE or greater turbulence events in which a pair of diagnostics each reached significant thresholds. Generally, there is little overlap indicating that the diagnostics are relatively independent of each other. The major exception is that low Ri_E and high wind shear do occur quite often together, as expected since the wind shear squared is the denominator of the Richardson number. Another pair that may be related are the divergence tendency and the environmental Richardson number. On several occasions pressure level maps computed at the AWC showed contours of divergence tendency and Ri_E nearly overlapping. A third interesting relatively high pairing is anticyclonic instability and unbalanced ageostrophic wind.

Table 3. Percentages of Table 2 diagnostics at subjectively chosen thresholds that occurred together when the turbulence report was MODERATE or greater. The table reads, "the percentage of the column diagnostic that also occurred when the row diagnostic occurred."

	Inadwind>25	Uagewind>25	Divgtend>15	AI<0	Ri_E<I	$Wshr^2$>.0005
Inadwind>25	—	.37	.19	.02	.27	.15
Uagewind>25	.35	—	.16	.13	.19	.13
Divgtend>15	.20	.18	—	.04	.44	.31
AI<0	.04	.33	.08	—	.16	.08
Ri_E<1	.14	.11	.21	.04	—	.28
$Wshr^2$>.0005	.16	.15	.25	.04	.58	—

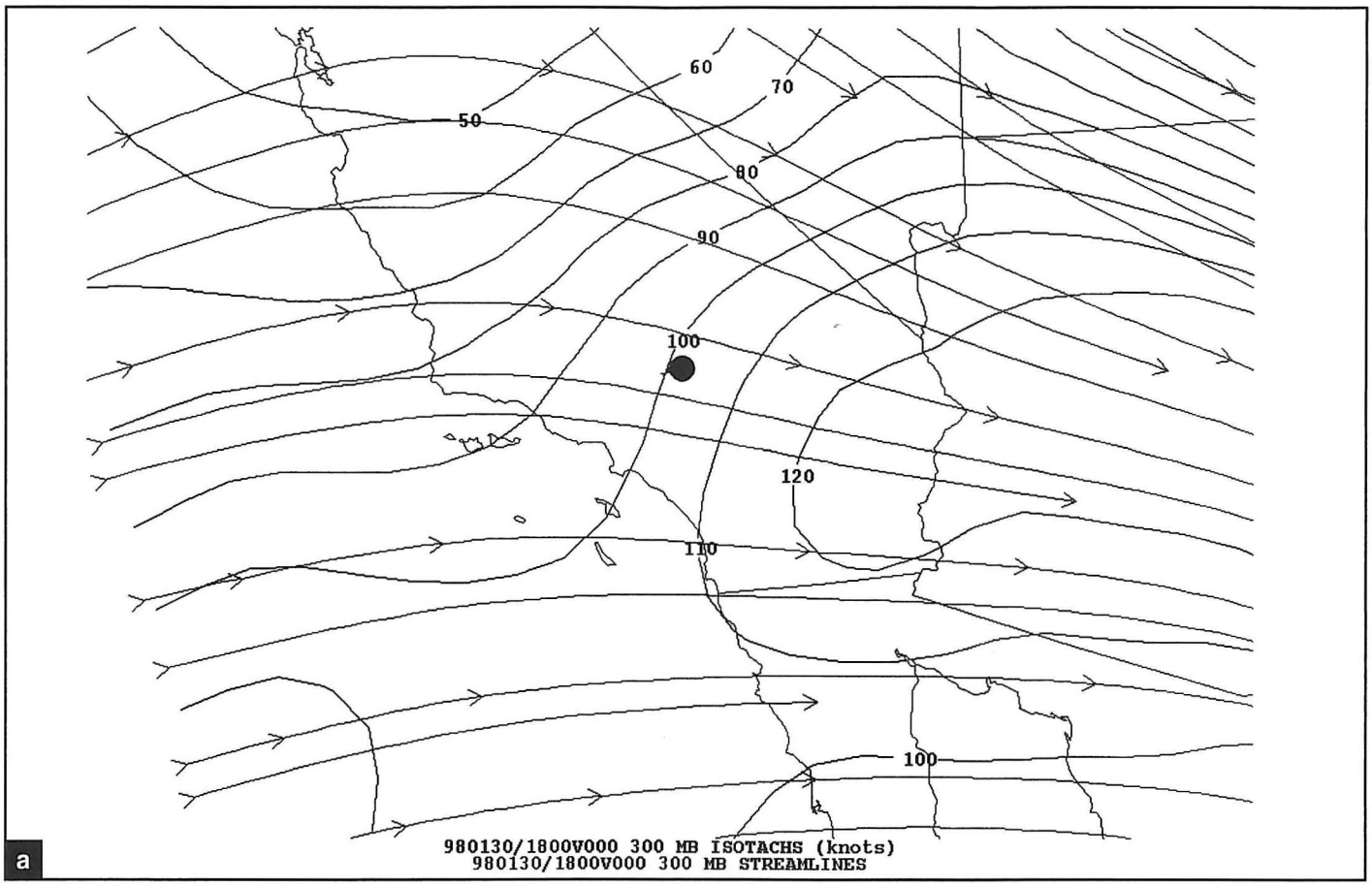
60
70
50
80
90
100
120
110
100
980130/1800V000 300 MB ISOTACHS (knots)
980130/1800V000 300 MB STREAMLINES

a

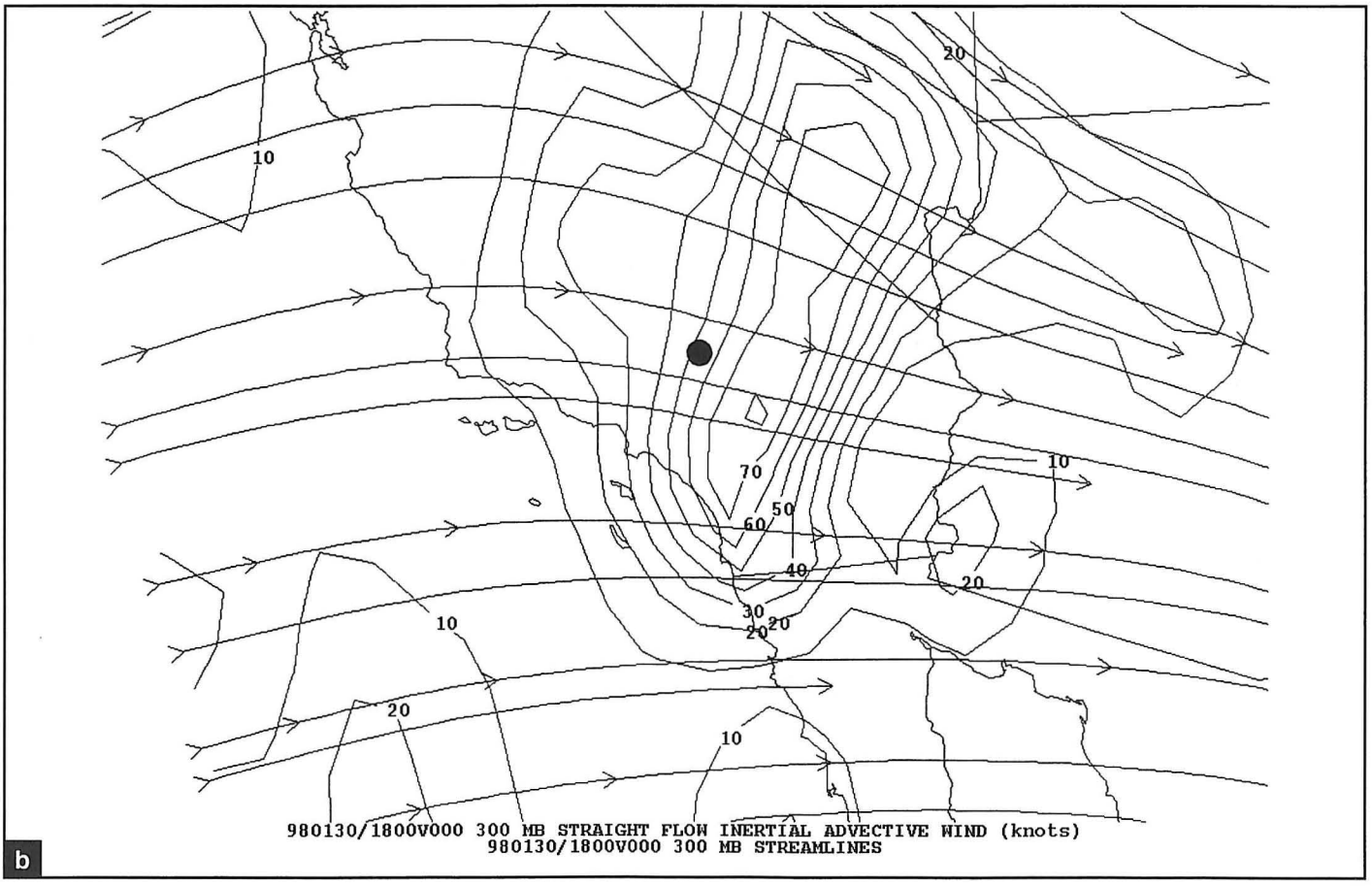
20
10
10
70
50
60
40
20
30
20
20
10
20
10
980130/1800V000 300 MB STRAIGHT FLOW INERTIAL ADVECTIVE WIND (knots)
980130/1800V000 300 MB STREAMLINES

b

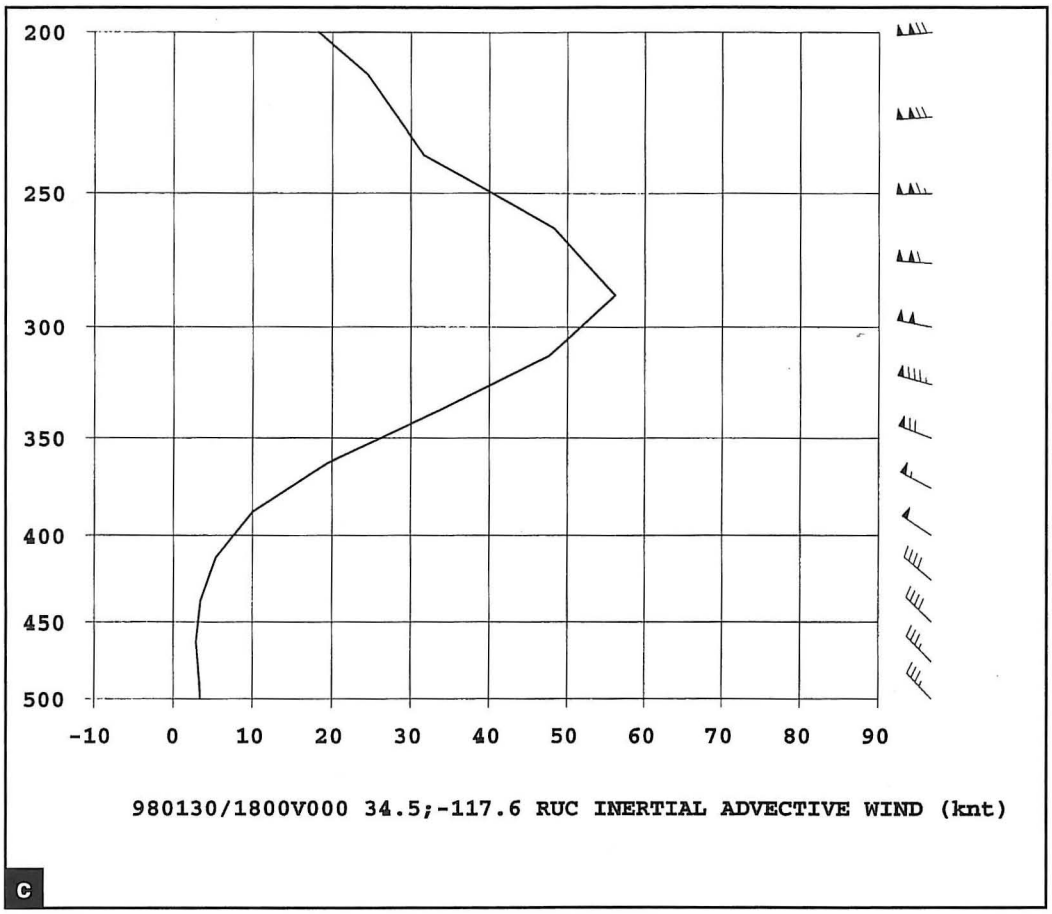

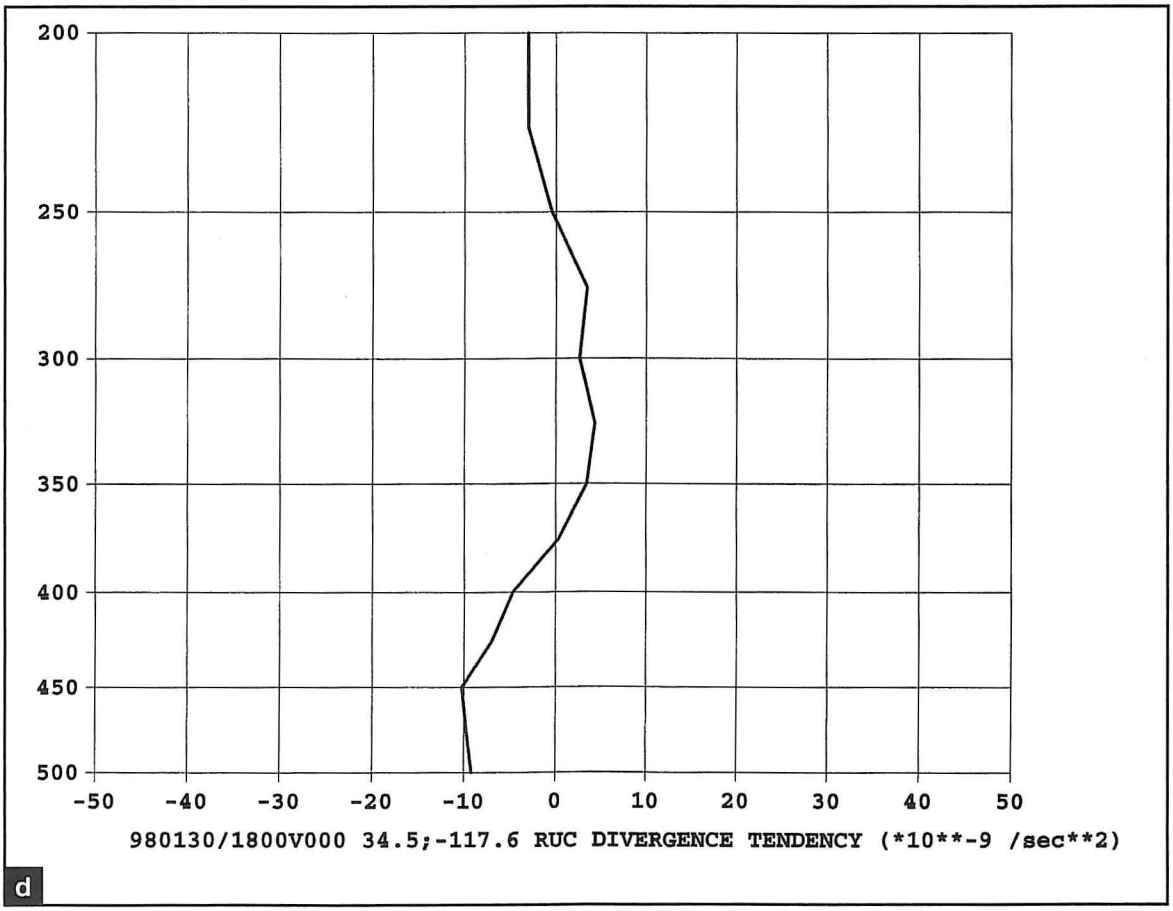

Fig. 6. a) RUC 300-mb streamlines and isotachs for 1800 UTC 30 January 1998 over southern California. b) RUC 300-mb streamlines and inertial advective wind. (See Table 1 for definition.) c) Same as Fig. 2 except a profile of the inertial advective wind. d) Same as Fig. 2 except a profile of the divergence tendency. The dark circle in a) and b) locates the aircraft position at 1806 UTC 30 January 1998.

What about the pilot report in Section 3? Figure 6 shows selected synoptic aspects of this case. The vertical profile of the inertial advective wind in Fig. 6c showed that it exceeded 50 knots (26 m s^{-1}) from about 29,000 ft to 32,000 ft, precisely the layer in which the aircraft experienced the turbulence. The vertical profile of divergence tendency in Fig. 6d showed the highest values in this layer and slightly below this layer but the absolute values were low compared with Table 3 values. The flow in all layers was not anticyclonic enough to be unstable according to the formula for anticyclonic instability. Gravity waves from other sources were unlikely since there was no convection in the area and the flow profile was not favorable with the underlying terrain for mountain waves. Therefore, given all the data from this case, the turbulence event was probably caused by a gravity wave which probably resulted from unbalanced flow.

5. Conclusions

There is ample theory showing that gravity waves can cause turbulence through the modification of the environmental Richardson number to a local Richardson number less than the critical Richardson number for turbulence. The theory allows for a Prandtl number in the TKE equation to approach or equal the critical Richardson number, thereby reducing the uncertainty of turbulence occurrence. The theory supports observations by Beckman (1981) and others who have connected wave clouds on satellite images with CAT reports.

The respective theoretical roles of environmental wind shear, Richardson number, and unbalanced flow suggest an ingredients-based CAT forecast technique similar to thunderstorm forecasting (Doswell et al, 1996). Environmental layers favorably setup with high wind shear and low Richardson number should be given first consideration. In these layers only minimal gravity wave forcing is necessary to trigger CAT. Regions of highly unbalanced flow may produce high amplitude gravity waves sufficient by themselves to produce CAT.

The governing TKE equations to quantify this technique are (2) combined with (4) and (5) or (3) combined with (6). *The problem is to find the non-dimensional amplitudes (â) of unbalanced flow waves.* Knowing â, one can compute the maximum TKE production from the local modifications to the wind shear and stability. Section 3 defined â in terms of two environmental variables, stability and wind speed, and two wave variables, the actual wave amplitude and the wave phase velocity.

Theoretically and observationally, two questions remain. 1) What are the amplitudes and phase velocities of unbalanced flow waves? In the case of the B767 ascent out of Los Angeles, there was unbalanced flow diagnosed, and the aircraft winds reported were sufficient to estimate â. This was a rare pilot report. A successful turbulence diagnostic for everyday use by AWC forecasters will have to make good estimates of â.

2) What are the best diagnostics for unbalanced flow? The unbalanced flow diagnostics presented in Section 3 are not statistically correlated with each other in the AWC turbulence pilot report database, implying more than one process can cause unbalanced flow. Ongoing research at the AWC is aimed at developing better diagnostics. Ultimately, since the horizontal forces on air parcels in these cases are unbalanced by definition, there may very well be a single universal diagnostic that will work well.

While this paper emphasized unbalanced flow as a cause of gravity waves, it is not the only one. Because of numerous other causes, the analysis of gravity wave sources in an operational environment is going to be very complex. Furthermore, wave-mean flow and wave-wave interactions (Franke and Robinson 1999) add more levels of complexity.

Finally, although it appears that gravity waves are significant triggers of CAT, it is much too premature to conclude that they are an exclusive cause of CAT. There may be other mechanisms that locally modify wind shears and stabilities so that CAT may form.

Acknowledgments

Many thanks go to John Knox whose feedback on this paper and my work in general has been the basis for any success I can claim. Roy Darrah and Robert Sharman also gave me valuable reviews.

References

Alaka, M.A., 1961: The occurrence of anomalous winds and their significance. *Mon. Wea. Rev.*, 89, 482-494.

Beckman, S.K., 1981: Wave clouds and severe turbulence. *Natl. Wea. Dig.*, 6:3, 30-37.

Blumen, W., 1972: Geostrophic adjustment. *Rev. Geophys. Space Phys.*, 10, 485-528.

Browning, K.A., T.W. Harrold, and J.R. Starr, 1970: Richardson number limited shear zones in the free atmosphere. *Quart. J. Roy. Met. Soc.*, 96, 40-49.

Cahn, A., 1945: An investigation of the free oscillations of a simple current system. *J. Meteor.*, 2, 113-119.

Charney, J., 1955: The use of the primitive equations of motion in numerical prediction. *Tellus*, 7, 22-26.

Cundy, R.G., 1999: Use of numerical guidance aids in forecasting a turbulence superoutbreak over the eastern United States. *Proc. Eighth Conf. on Aviation, Range, and Aerospace Meteorology*, Dallas TX, Amer. Meteor. Soc., 382-386.

Doswell, C.A. III, H.E. Brooks, and R.A. Maddox, 1996: Flash flood forecasting: An ingredients based methodology. *Wea. Forecasting*, 11, 560-581.

Duffy, D.G., 1990: Geostrophic adjustment in a baroclinic atmosphere. *J. Atmos. Sci.*, 47, 457-473.

Dunkerton, T.J., 1997: Shear instability of inertia-gravity waves. *J. Atmos. Sci.*, 54, 1628-1641.

Dutton, J.A., and H.A. Panofsky, 1970: Clear air turbulence: A mystery may be unfolding. *Science*, 167, 937-944.

Dutton, M.J.O., 1980: Probability forecasts of clear-air turbulence based on numerical model output. *Meteorological Magazine*, 109, 293-309.

Ellrod, G.P., and D.I. Knapp, 1992: An objective clear-air turbulence forecasting technique: Verification and operational use. *Wea. Forecasting,* 7, 150-165.

Franke, P.M. and W.A. Robinson, 1999: Nonlinear behavior in the propagation of atmospheric gravity waves. *J. Atmos. Sci.*, 56, 3010-3027.

Fritts, D.C., and Z. Luo, 1992: Gravity wave excitation by geostrophic adjustment of the jet stream. Part 1: Two-dimensional forcing. *J. Atmos. Sci.*, 49, 681-697.

Garratt, J.R., 1992: *The Atmospheric Boundary Layer*. Cambridge University Press, 316 pp.

Kaplan, M.L., S.E. Koch, Y.L. Lin, R.P. Weglarz, and R.A. Rozumalski, 1997: Numerical simulations of a gravity wave event over CCOPE. Part 1: The role of geostrophic adjustment in mesoscale jetlet formation. *Mon. Wea. Rev.*, 125, 1185-1211.

Kennedy, P.J., and M.A. Shapiro, 1980: Further encounters with clear air turbulence in research aircraft. *J. Atmos. Sci.*, 37, 986-993.

Knox, J.A., 1997a: Generalized nonlinear balance criteria and inertial stability. *J. Atmos. Sci.*, 54, 967-985.

_____ , 1997b: Possible mechanisms of clear-air turbulence in strongly anticyclonic flows. *Mon. Wea. Rev.*, 125, 1251-1259.

Koch, S.E., and P.B. Dorian, 1988: A mesoscale gravity wave event observed during CCOPE. Part III: Wave environment and probable source mechanism. *Mon. Wea. Rev.*, 116, 2570-2592.

Kondo, J., O. Kanechika, and N. Yasuda, 1978: Heat and momentum transfers under strong stability in the atmospheric surface layer. *J. Atmos. Sci.*, 35, 1012-1021.

Lester, P.F. and W.A. Fingerhut, 1974: Lower turbulent zones associated with mountain lee waves. *J. Appl. Meteor.*, 13, 54-61.

MacCready, P.B., 1964: Standardization of gustiness values from aircraft, *J. Appl. Meteor.,* 3, 439-449.

McCann, D.W., 1999: A simple turbulent kinetic energy equation and aircraft boundary layer turbulence. *Natl. Wea. Dig.*, 23:1-2, 13-19.

Mellor, G.L., and T. Yamada, 1982: Development of a turbulent closure model for geophysical fluid problems. *Rev. Geophys. Space Phys.*, 20, 851-875.

Miles, J. W., and L.N. Howard, 1964: Note on a heterogeneous flow. *J. Fluid Mech.*, 20, 331-336.

Murphy, E.A., R.B. D'Agostino, and J.P. Noonan, 1982: Patterns in the occurrences of Richardson numbers less than unity in the lower atmosphere. *J. Appl. Meteor.*, 21, 321-333.

O'Sullivan, D. and T.J. Dunkerton, 1995: Generation of inertia-gravity waves in a simulated life cycle of baroclinic instability. *J. Atmos. Sci.*, 52, 3695-3716.

Palmer, T.N., G.J. Shutts, and R. Swinbank, 1986: Alleviation of a systematic westerly bias in general circulation and numerical weather prediction models through an orographic gravity wave drag parameterization. *Quart. J. Roy. Met. Soc.*, 112, 1001-1039.

Reed, R.J. and K.R. Hardy, 1972: A case study of persistent, intense, clear air turbulence in an upper level frontal zone. *J. Appl. Meteor.*, 11, 541-549.

Roach, W.T., 1970: On the influence of synoptic development on the production of high level turbulence. *Quart. J. Roy. Met. Soc.*, 96, 413-429.

Rockey, C., and D.W. McCann, 1995: Turbulent kinetic energy production in significant turbulence events. *Proc. Sixth Conf. on Aviation Weather Systems*, Dallas TX, Amer. Meteor. Soc., 166-169.

Rossby, C.G., 1938: On the mutual adjustment of pressure and velocity distributions in simple current systems, Part II. *J. Mar. Res.*, 1, 239-263.

Schwartz, B., 1996: The quantitative use of PIREPs in developing aviation weather guidance products. *Wea. Forecasting*, 11, 372-384.

_____ , and S.G. Benjamin, 1995: A comparison of temperature and wind measurements from ACARS-equipped aircraft and rawinsondes. *Wea. Forecasting*, 10, 528-544.

Thorpe, S.A., 1969: Experiments on the stability of stratified shear flows. *Radio Sci.*, 4, 1327-1331.

Uccellini, L.W., P.J. Kocin, R.A. Petersen, C.H. Wash, and K.F. Brill, 1984: The President's Day cyclone of 18-19 February 1979: Synoptic overview and analysis of the subtropical jet streak influencing the pre-cyclogenetic period. *Mon. Wea. Rev.*, 112, 31-55.

_____, and S.E. Koch, 1987: The synoptic setting and possible energy sources for mesoscale wave disturbances. *Mon. Wea. Rev.*, 115, 721-729.

van Tuyl, A.H., and J.A. Young, 1982: Numerical simulation of nonlinear jet streak adjustment. *Mon. Wea. Rev.*, 110, 2038-2054.

Vinnichenko, N.K., N.Z. Pinus, S.M. Shmeter, and G.N. Shur, 1980: *Turbulence in the Free Atmosphere*, Consultants Bureau, 310 pp.

Weglarz, R.P., and Y-L Lin, 1997: A linear theory for jet streak formation due to zonal momentum forcing in a stably stratified atmosphere. *J. Atmos. Sci.*, 54, 908-932.

Zack, J.W., and M.L. Kaplan, 1987: Numerical simulations of the subsynoptic features associated with the AVE-SESAME I case. Part 1. The preconvective environment. *Mon. Wea. Rev.*, 115, 2367-2394.

Appendix

List of Symbols

a	gravity wave amplitude
$\hat{a}$	non-dimensional gravity wave amplitude
c	gravity wave phase velocity
D	horizontal divergence of the wind
f	Coriolis parameter
g	acceleration due to gravity
J	Jacobian operator
K_h	eddy thermal diffusivity
K_m	eddy viscosity
N	stability
Pr	Prandtl number (K_m/ K_h)
Ri	Richardson number
Ro	Rossby number
t	time
u	x-component of the wind
V	mean horizontal wind
v	y-component of the wind
V_{ag}	ageostrophic wind
V_g	geostrophic wind
V_{inad}	inertial advective wind
V_{uage}	unbalanced ageostrophic wind
z	vertical coordinate
β	change in Coriolis parameter with latitude
ϵ	rate of turbulent kinetic energy dissipation
Φ	geopotential height
ϕ	gravity wave phase angle
Θ_v	mean virtual potential temperature
ζ	relative vorticity
ζ_{curv}	curvature component of relative vorticity ($\|V\|/r$, where r is radius of curvature of a trajectory)
$\bullet\bullet E$	quantity measured in the environment
$\bullet\bullet L$	quantity locally modified